Synthesis of TiO_2 *via* Modified Sol-gel Method and its Use in Carbonized Medium-density Fiberboard for Toluene Decomposition

Min Lee,[a] Sang-Bum Park,[a] and Sung-Phil Mun [b,*]

A solution-type TiO_2-based photocatalyst for the decomposition of volatile organic compounds was synthesized using a modified sol-gel method under either alcohol (ethanol or isopropanol) or aqueous conditions. Anatase-type TiO_2 was successfully synthesized with additional hydrothermal treatment using either type of medium. However, the aqueous condition for TiO_2 synthesis was more convenient for the formation of anatase-type TiO_2. Based on X-ray diffraction analysis data, the optimal hydrothermal treatment temperature was 80 °C for anatase-type TiO_2 formation; at temperatures below 80 °C or above 90 °C, mostly rutile-type TiO_2 was formed. The synthesized anatase-type TiO_2 solution was applied to the surface of carbonized medium-density fiberboard (c-MDF). The anatase-type TiO_2 on c-MDF showed good maintenance of toluene decomposition performance even after repeated use for 14 weeks.

Keywords: Toluene; Decomposition; TiO_2; Carbonization; Medium-density fiberboard

*Contact information: a: Department of Forest Products, National Institute of Forest Science, Seoul, South Korea; b: Department of Wood Science and Technology, Chonbuk National University, Jeonju, South Korea; *Corresponding author: msp@jbnu.ac.kr*

INTRODUCTION

As industrialization and urbanization have progressed rapidly since the third industrial revolution, pollution of the urban environment has become increasingly severe due to urban concentration and increases in industrial facilities and traffic volumes (Field 2010). In addition, with economic improvements and changes in living and working styles, modern people usually spend more than 90% of their time indoors (US EPA 2010). Therefore, the effect of indoor environments on human health has increased (CDC 2006). Indoor air quality problems have begun to increase with the closure of buildings and the installation of artificial energy-decomposition devices used to improve energy efficiency in various industries (Kim 1999; Spengler *et al*. 2006). Recently, populations vulnerable to environmental illnesses, such as the elderly, children, and pregnant women, have increasingly suffered from atopy and asthma (US EPA 2010).

In the last decade, nanostructured materials have received great interest for catalysis and other applications because of their unique texture and structural properties (Molinari *et al*. 2000; Ao and Lee 2004; Guo *et al*. 2004; Hashimoto *et al*. 2005). Many studies have focused on metal oxides such as TiO_2, SnO_2, VO_2, and ZnO (Torimoto *et al*. 1997; Fujishima *et al*. 2000). Titanium dioxide has received research attention due to its chemical structure and biocompatibility as well as its physical, optical, and electrical properties (Takeda *et al*. 1995; Doi *et al*. 2000; Tokoro and Saka 2001; Varghese *et al*. 2003; Wen *et al*. 2005). Photocatalytic reactions are widely used for various environmental purification purposes, such as the

decomposition of contaminants in water and air (Andersson *et al*. 2002; Wahi *et al*. 2006; Wu and Qi 2007). When TiO_2 is used as a photocatalyst, it has three crystal structures, classified as anatase, rutile, and brookite. The low-formation-temperature anatase-type and high-formation-temperature rutile-type are commonly found. Although the two structures have similar tetragonal symmetry, in the rutile crystal structure, the octahedral structures with Ti centers share oxygen atoms at the vertex positions; in the anatase-type, the octahedral structures share edges. Because of these structural differences, the two phases exhibit different physical and chemical properties. To synthesize nanostructured TiO_2, the sol-gel process, direct oxidation, chemical vapor deposition, electrodeposition, an ultrasonic chemical method, and a microwave method have been used (Zhang and Gao 2003; Corradi *et al*. 2005; Wang *et al*. 2009; Xue *et al*. 2011; Bazargan *et al*. 2012; Byranvand *et al*. 2013; Zhou *et al*. 2013). Photocatalysts prepared *via* the sol-gel method are typically applied as coating agents through spin-coating or spraying.

Kercher and Nagle (2002) introduced carbonized boards by pyrolyzing wood-based panels at high temperatures; they were intended for use as fuel cell membranes. The initial carbonized board was prepared at the laboratory scale of approximately 10 cm in size. In 2009, a crack- and twist-free carbonized board was developed by using medium-density fiberboard (MDF), plywood, and wood panels (Park *et al*. 2009). The physicochemical properties and functionality of carbonized MDF (c-MDF) have been investigated (Zhou *et al*. 2013; Lee *et al*. 2014; Lee *et al*. 2017a,b). The c-MDF can easily remove formaldehyde (a major volatile compound contributing to sick house syndrome) and shows some ability to remove other aromatic volatile organic compounds (VOCs), such as toluene and xylene, from indoor atmospheres (Park *et al*. 2009).

In this study, to improve the decomposition ability of c-MDF, a nano-sized TiO_2 photocatalyst was prepared by using the modified sol-gel synthetic method, and then it was applied to prepared c-MDF to provide photocatalytic function. The anatase-type TiO_2 sol-applied c-MDF was then investigated to confirm enhancement of the photocatalytic decomposition ability for toluene.

EXPERIMENTAL

Materials

The MDF (0.64 g/cm^2, E_1 grade) was purchased from Sunchang Industry (Incheon, Korea).

Titanium tetrapropoxide (Ti-tip) and titanium tetrachloride ($TiCl_4$; DaeJung Chemicals & Metals Co., Ltd., Siheung-si, Gyeonggi-do, Korea) were used as photocatalyst precursors for the synthesis of TiO_2. The synthesis was performed in the presence of HCl (1 mol/L, Showa Chemical Industry Co., Ltd., Tokyo, Japan), NH_4OH (DaeJung Chemicals & Metals Co., Ltd., Siheung-si, Gyeonggi-do, Korea), NaOH (Duksan Pure Chemical Co., Ltd., Seoul, Korea), isopropyl alcohol (IPA; DaeJung Chemicals & Metals Co., Ltd., Siheung-si, Gyeonggi-do, Korea), and ethyl alcohol (99.5%, EtOH; Duksan Pure Chemical Co., Ltd., Seoul, Korea).

Standard TiO_2 (mixture of rutile and anatase types, nanopowder, < 100 nm) was purchased from Sigma-Aldrich (St. Louis, MO, USA).

Methods

Preparation of c-MDF

The MDF, which is a raw material for manufacturing the photocatalytic c-MDF, was cut into samples measuring 130 cm × 260 cm × 1.2 cm (W × L × T) and then wrapped in newspaper and aluminum foil according to Park's method (2009). The prepared MDF was stacked between graphite plates in a heat resistant box and then placed in an electric furnace. The carbonization program used a heating rate of 50 °C/h and a maximum temperature of 600 °C, which was held for 2 h followed by natural cooling (Park *et al.* 2009).

Synthesis of TiO_2-sol using alcohols

The Ti-tip was used as a photocatalyst precursor to synthesize the sol-type photocatalyst using alcohol (either EtOH or IPA) as the solvent (Fig. 1). In an Erlenmeyer flask (1 L), 340 g of the selected alcohol and 20 g of Ti-tip were mixed to prepare Solution 1. To prepare Solution 2, distilled and deionized (DI) water (80 g) and concentrated hydrochloric acid (5 g) were mixed in 340 g of alcohol (EtOH or IPA) and placed in a separatory funnel. Solution 2 from the separatory funnel was added dropwise at 60 drops/min to Solution 1 while it was stirred in an ice bath. The mixing of Solution 1 and Solution 2 continued for 3 h with an additional 1 h of stirring. To replace the alcohols with DI water, centrifugation was performed at 6,000 rpm (652 G-force) for 20 min at 10 °C. After decantation, 400 mL of DI water was added to the precipitate, followed by ultrasonic treatment (10 min) for dispersion. The TiO_2 dispersed in the DI water was refluxed at 80 °C for 1 h.

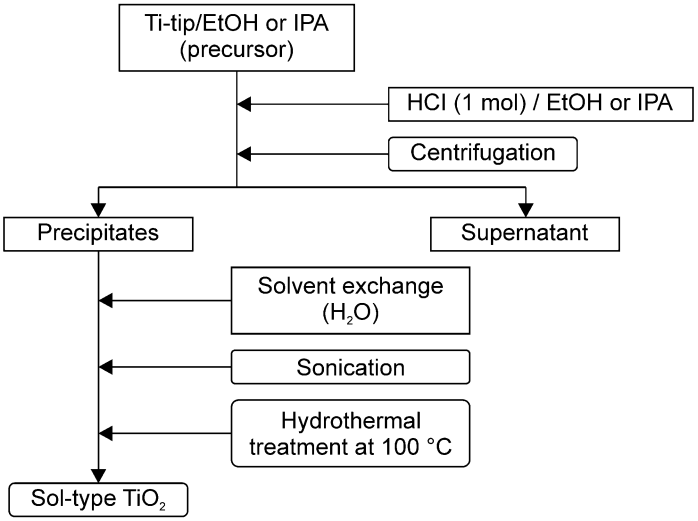

Fig. 1. Flow chart of sol-type TiO_2 preparation using alcohols

Synthesis of sol-type TiO_2 using water

The $TiCl_4$ was used as a photocatalyst precursor to synthesize a sol-type photocatalyst under an aqueous condition. Approximately 19 g of $TiCl_4$ was placed in an Erlenmeyer flask (1 L) and cooled in iced water. The DI water (200 mL) was slowly added dropwise to the cooled $TiCl_4$ solution to prepare a 0.5 M $TiOCl_2$ aqueous solution. A 5 M NH_4OH aqueous solution was added dropwise for approximately 10 min to the prepared 0.5 M $TiOCl_2$ aqueous solution to obtain the TiOH precipitate as a reaction product. To remove Cl ions from the TiOH precipitate, it was washed three times with DI water and the supernatant was removed *via*

centrifugation. The conditions for centrifugation were 6,000 rpm (652 G-force) for 20 min at 10 °C. The washed TiOH was dispersed *via* sonication for 10 min in 200 mL of 5 M NaOH solution. The aqueous solution of NaOH in which TiOH was dispersed was thermally treated at reaction temperatures ranging from 50 °C to 100 °C for 1 h, as well as at room temperature (25 °C). The supernatant was removed through centrifugation. The resulting precipitate was treated in 200 mL of 0.5 M HCl solution at 60 °C for 24 h with occasional shaking. After treatment, the suspension was centrifuged under the same conditions mentioned above. The resulting TiO_2 was subsequently repeatedly washed with DI water until the pH reached 7.0. The washed TiO_2 was dispersed in 200 mL of DI water through ultrasonication for 10 min (Fig. 2).

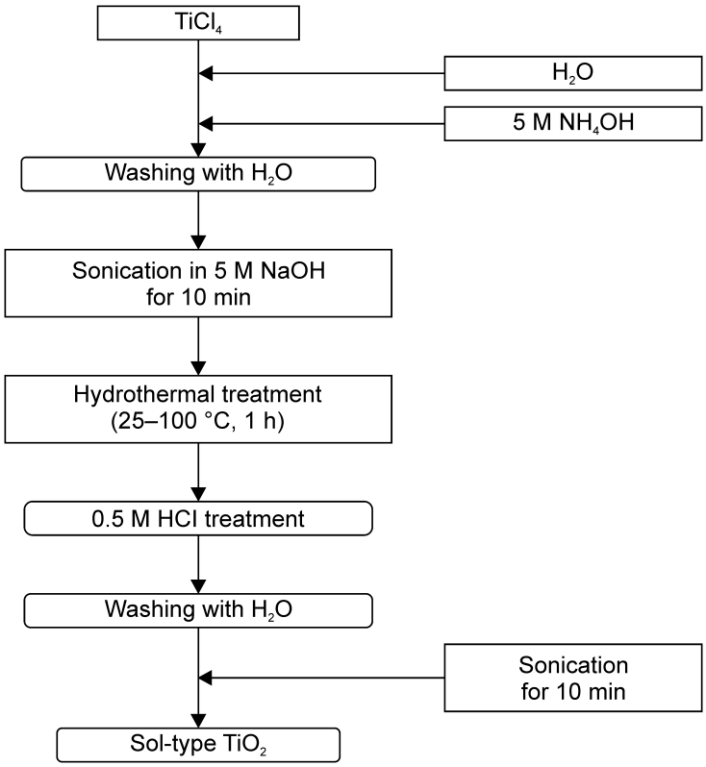

Fig. 2. Flow chart of sol-type TiO_2 preparation using water

Crystallinity of TiO_2

X-ray diffraction (XRD; X'pert Powder; Malvern Panalytical Ltd., Malvern, United Kingdom) was used to confirm the crystal form of TiO_2. The synthesized sol-type TiO_2 was dried and finely ground in an agate mortar and then placed in a sample holder. The holder was mounted, and the sample was measured at 2θ values from 15° to 80° at 40 kV and 30 mA. All spectra obtained were normalized and then used.

Microscopic analysis of sol-type TiO_2/c-MDF

After the synthesis of sol-type TiO_2-treated c-MDF (sol-type TiO_2/c-MDF), a scanning electron microscope (SEM, JSM 6400; JEOL Ltd., Tokyo, Japan) and energy-dispersive spectroscopy (EDS, JED-2300; JEOL Ltd., Tokyo, Japan) were performed to determine the Ti distribution on the surface of the c-MDF. To analyze the particle size of the synthesized TiO_2, a spherical aberration-corrected transmission electron microscopy (TEM, JEM-ARM 200F;

JEOL Ltd., Tokyo, Japan) was used. The sample grid was immersed in a 1/10 diluted TiO_2-sol in IPA. The grid was then dried on a hot plate to remove the solvent. Before analysis, the dried grid was pretreated by an ion cleaner (EC-52000IC, JEOL Ltd., Tokyo, Japan) for 10 min. The acceleration voltage used was 200 kV and the lattice resolution was 0.2 nm.

Toluene decomposition performance

A sol-type TiO_2/c-MDF (300 cm^2) was placed in a 20-L stainless steel chamber that was filled with 20-ppm toluene standard gas three times to evaluate the toluene decomposition performance. A Tedlar bag (25-L, TP-25; TRS Environment™, Chesterfield, MI, USA) filled with nitrogen was connected to one of the inlets at the bottom of the chamber. The concentration of toluene in the chamber was monitored at 0 h, 1 h, 3 h, 5 h, 7 h, and 9 h after the chamber was irradiated with ultraviolet (UV) radiation with wavelengths of 360 nm. A 1.0 L sample of air was collected in a Tenax-TA adsorption tube (Supelco Inc., Bellefonte, PA, USA) at a flow rate of 167 mL/min and then analyzed with a gas chromatograph-mass spectrometer (GC-MS, QP2010; Shimadzu, Kyoto, Japan). The analysis conditions are shown in Table 1.

Table 1. GC-MS and TD Analysis Conditions

TD-20 (Shimadzu, Kyoto, Japan)		GC/MS (QP2010; Shimadzu, Kyoto, Japan)	
List	Condition	List	Condition
Desorption temperature	280 °C	GC Column	VB-1 (0.32 mm × 60 m × 1 μm)
Desorption time	15 min	Initial	40 °C, 5 min
Cold trap temperature	−10 °C	1st ramp	10 °C/min, 80 °C, 16 min
2nd desorption temperature	300 °C	2nd ramp	20 °C/min, 200 °C, 4 min
Cold trap hold time	15 min	Column flow	1 mL/min
Cold trap packing	Tenax TA	MS source temp.	200 °C
Split	1:10	Detector type	EI (Quadrupole)
Valve temperature	210 °C	Mass range	35 amu to 350 amu
Transfer line temperature	250 °C	Electron energy	70 eV

RESULTS AND DISCUSSION

Sol-type TiO_2 Synthesized Using Alcohols

Sol-type TiO_2 synthesis

The final concentrations of sol-type TiO_2 synthesized using lower alcohols (IPA and EtOH) were 0.71% and 0.72%, respectively. After the preparation of sol-type TiO_2 by IPA or EtOH, TiO_2 appeared to be well dispersed. However, after standing overnight, precipitates were observed in the TiO_2 synthesized using IPA as the solvent, which would impede spraying. The TiO_2 synthesized in EtOH remained well dispersed after standing overnight (Fig. 3).

Crystallinity of sol-type TiO_2 synthesized in alcohols

The X-ray diffraction analysis of TiO_2 synthesized using alcohols as solvents showed anatase-type TiO_2 in both the solvents. However, the peak width and intensity in each sample

were wide and low, respectively (Fig. 4). Therefore, the crystallinity of TiO_2 may be very low in both sol-type photocatalysts. As previously mentioned in the TEM results, TiO_2 that was synthesized under these alcohol conditions was mostly amorphous in phase.

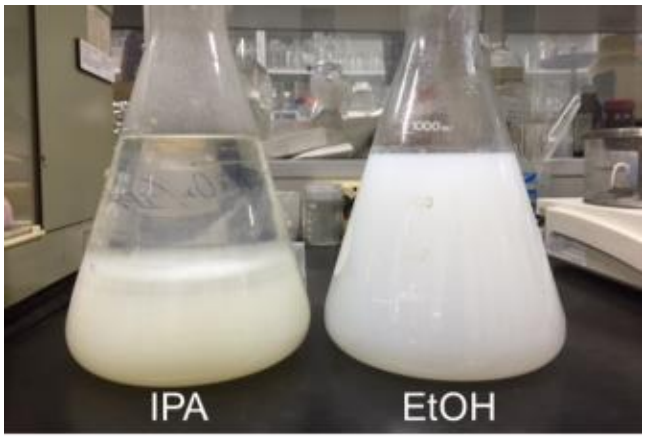

Fig. 3. Photos of sol-type TiO_2 synthesized in IPA and EtOH after 1 day

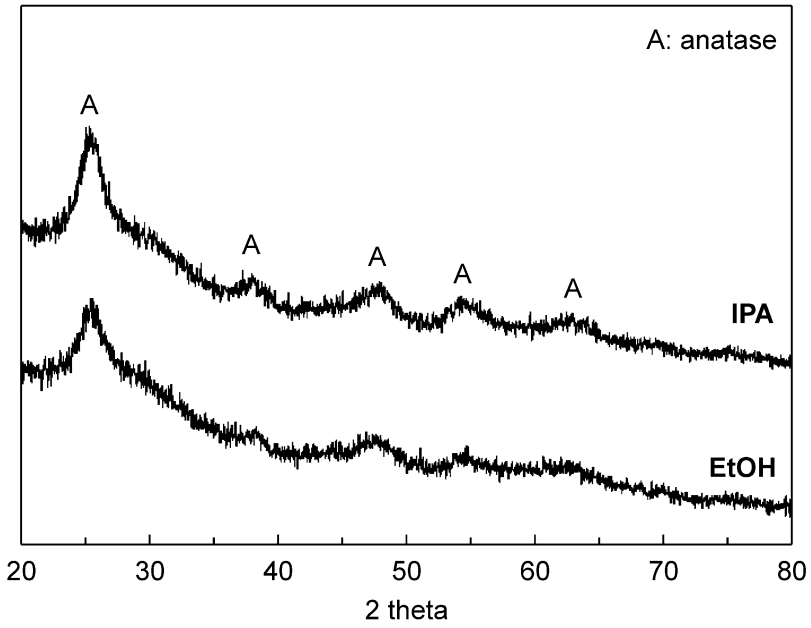

Fig. 4. XRD patterns of sol-type TiO_2 synthesized in IPA and EtOH

Crystallinity of hydrothermally treated sol-type TiO_2 synthesized in alcohols

The two types of alcohols, IPA and EtOH, used in the reaction were replaced with DI water, and then thermal treatment was conducted under refluxing conditions. As shown in Fig. 5, XRD data indicated that the amorphous form of TiO_2 was transformed into crystalline TiO_2. However, the peak width remained greater than that of the standard TiO_2 used as the standard sample. Therefore, low photocatalyst activity was expected. In addition, the synthesis of a sol-type photocatalyst using alcohols may be less economically efficient because additional processes of water substitution and thermal treatment are necessary.

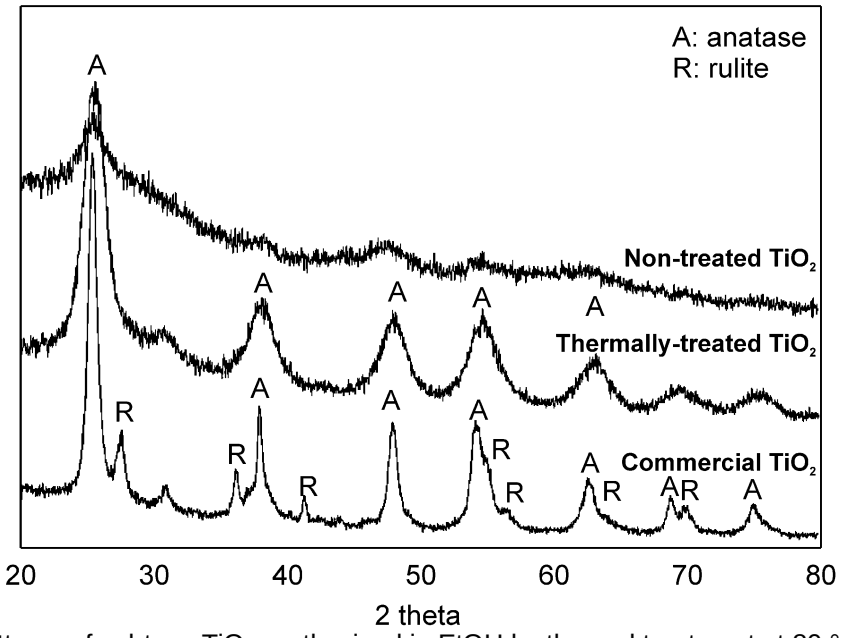

Fig. 5. XRD patterns of sol-type TiO_2 synthesized in EtOH by thermal treatment at 80 °C

Sol-type TiO_2 Synthesized with Water

Sol-type TiO_2 synthesis

The final concentration of the sol-type TiO_2 synthesized in water was 3.11%. In the syntheses using IPA and EtOH, phase separation was observed after TiO_2 preparation, followed by gelation as time passed. However, the sol-type TiO_2 synthesized using water as a solvent showed good dispersity, although some precipitates were observed 10 days after preparation (Fig. 6.).

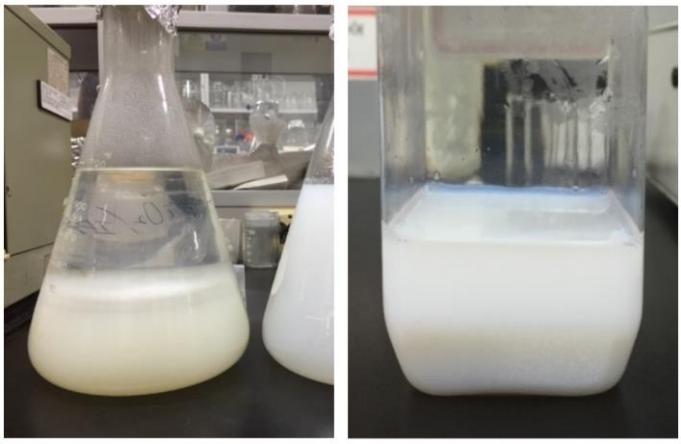

Fig. 6. Photos of synthesized sol-type TiO_2 (Left: IPA, right: DI water)

Microscopic observation of sol-type TiO_2 synthesized with water

Figure 7 shows TEM images of TiO_2 synthesized in water. The TiO_2 prepared by hydrothermal treatment at 80 °C showed spherical crystals; TiO_2 that was hydrothermally

treated at 100 °C showed acicular crystals. In general, anatase TiO_2 was spherical and rutile TiO_2 showed rod or needle forms (Fujishima *et al.* 2000; Hashimoto *et al.* 2005). The anatase-type TiO_2 was formed by hydrothermal treatment at 80 °C. The TiO_2 treated at 80 °C had an average length of 35 ± 11 nm and a width of 25 ± 12 nm. The TiO_2 treated at 100 °C had an average length of 72 ± 14 nm and a width of 14 ± 5 nm.

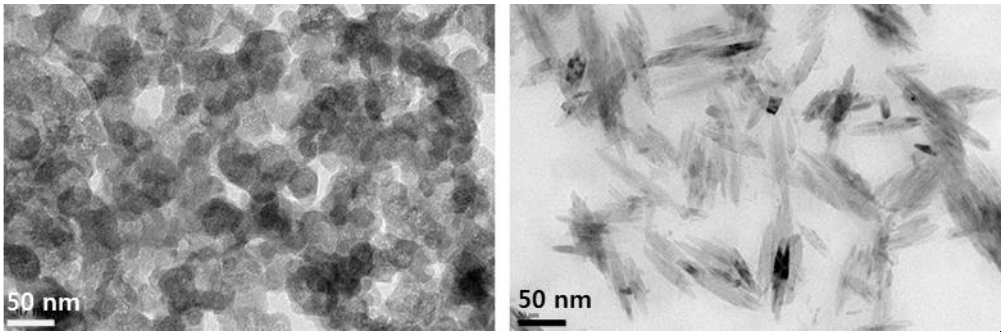

Fig. 7. TEM images of sol-type TiO_2 synthesized in water by hydrothermal treatment

Crystallinity of sol-type TiO_2 synthesized in water

During the alkali treatment that followed the ammonia water treatment, the effect of various temperatures on the crystal form changes of the sol-type TiO_2 was investigated. Particles of the sol-type photocatalyst alkali that was treated at room temperature appeared amorphous, similar to those of the photocatalysts prepared using alcohols. From Fig. 8, the amorphous phase of TiO_2 was transformed into a crystalline one with heating applied during the alkali treatment.

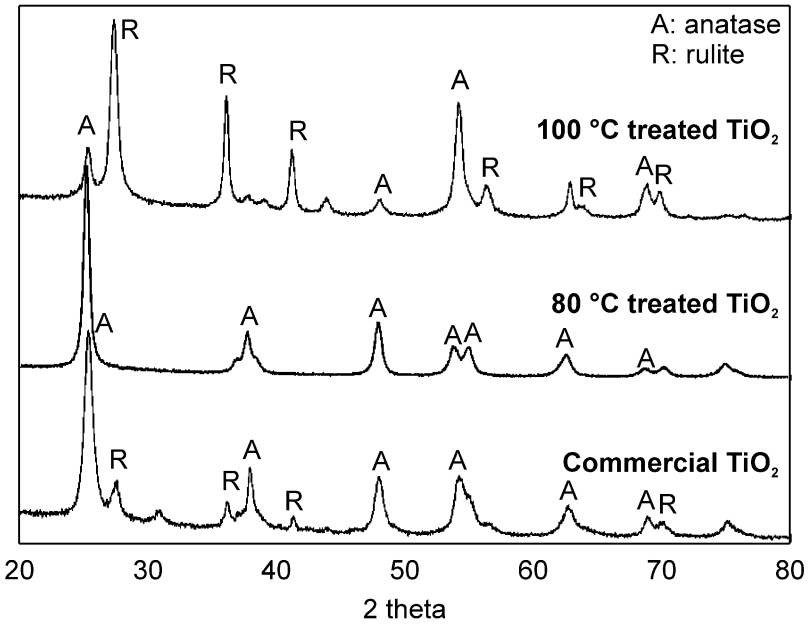

Fig. 8. XRD pattern of sol-type TiO_2 prepared at 80 °C and 100 °C

During treatment at 80 °C, all peaks related to rutile crystals in the XRD data disappeared, with only anatase crystal peaks remaining. With treatment at 90 °C or higher, the

anatase crystal peaks disappeared again and rutile crystals peaks appeared. These results indicated that 80 °C hydrothermal treatment was the optimum condition for synthesizing anatase-type TiO_2, which is known to have higher photocatalytic activities. Therefore, the hydrothermal conditions were critical in synthesizing the anatase form of the TiO_2 photocatalyst in water. In addition, XRD pattern of TiO_2 treated under 70 °C showed similar pattern to 100 °C treated TiO_2 (data not shown). Therefore, a mixture of anatase and rutile crystals of TiO_2 was formed with treatment at 50 °C to 70 °C. A spherical aberration-corrected TEM was used to observe the crystal lattice of TiO_2 obtained from the photocatalyst precursors Ti-tip and $TiCl_4$. The TiO_2 was shown to have a hexagonal close-packed structure, which is expected to have a face-centered cubic (FCC) lattice with 001 zone axis. Figure 9 shows the crystal lattice of sol-type anatase TiO_2 particles treated at 80 °C. The TiO_2 lattice dimension was 0.344 nm to the first point and 0.262 nm to the second point, confirming that the axis was 001 in an FCC lattice. These values were compared with Joint Committee on Powder Diffraction Standards (JCPDS) card values. The synthesized TiO_2 from water conditions with 80 °C hydrothermal treatment was thus confirmed as anatase-type through a spherical aberration-corrected TEM observation.

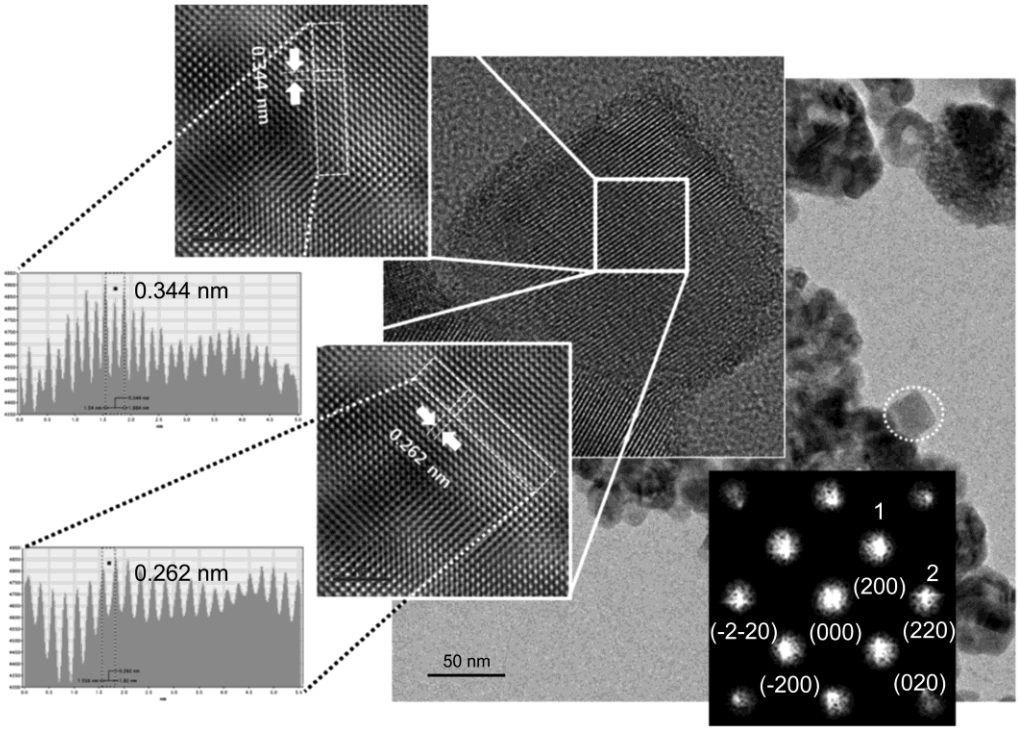

Fig. 9. A spherical aberration-corrected TEM data confirming crystal lattice of sol-type TiO_2 synthesized in water condition with 80 °C hydrothermal treatment (reference code: 98-020-2242)

Distribution of sol-type TiO_2 on c-MDF

The sol-type TiO_2 synthesized in water with hydrothermal treatment at 80 °C was brushed on the surface of the c-MDF, which was prepared at 600 °C for 2 h. The TiO_2 distribution was examined using SEM-EDS. Figure 10 showed the EDS data for Ti, which was distributed over the entire surface of the c-MDF. As shown in Table 2, the surface of the c-MDF was covered by TiO_2 with the ratio of Ti to O of approximately 2:1.

Table 2. Atomic and Mass Percentages of Ti, O, and C on c-MDF

	Mass (%)	Atomic (%)
Ti	6.45	1.72
O	4.04	3.22
C	89.51	95.06

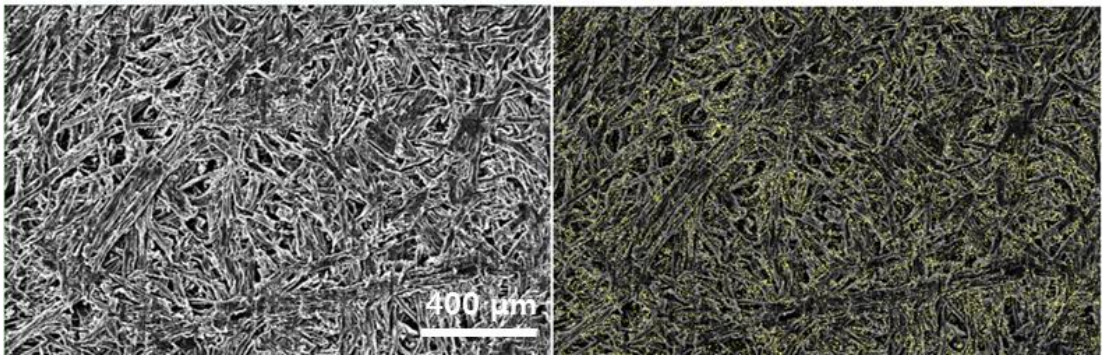

Fig. 10. Distribution of Ti (yellow dots) of sol-type TiO_2 on c-MDF

Toluene Decomposition Performance of Sol-type TiO_2/c-MDF

Ordinary c-MDF is known to have low removal performance for aromatic volatile compounds, such as toluene, xylene, and styrene (Park *et al*. 2009). Figure 11 shows the toluene decomposition performance of sol-type TiO_2 synthesized *via* hydrothermal treatment on c-MDF. The 80 °C-treated TiO_2 showed the highest toluene decomposition rate, while the toluene decomposition rate for the 100 °C-treated TiO_2 was lower than the 80 °C-treated TiO_2. However both specimens of TiO_2-treated c-MDF showed higher toluene decomposition rate than the blank samples and the samples that only used c-MDF.

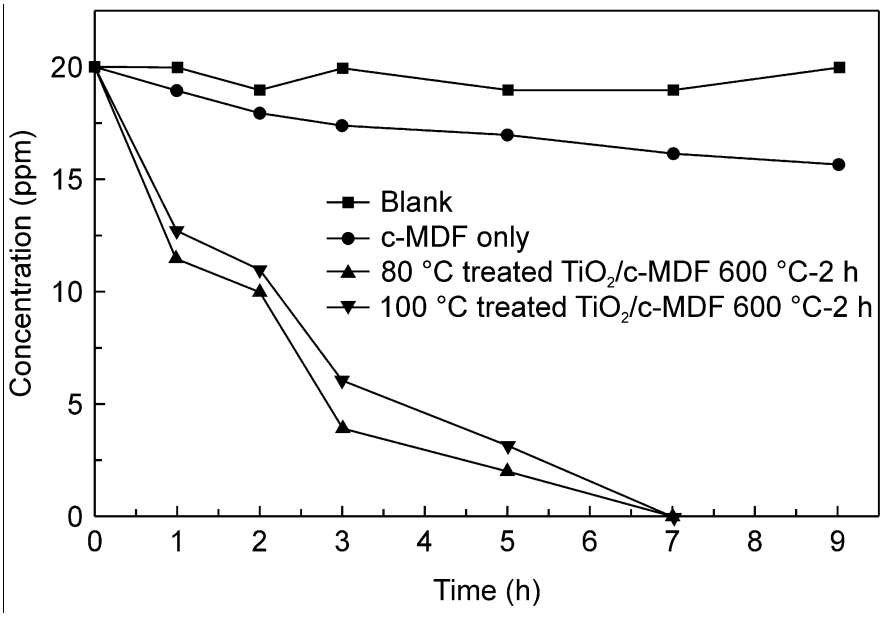

Fig. 11. Toluene decomposition of sol-type TiO_2 synthesized by 80 °C and 100 °C treatment on c-MDF and commercial sol-type TiO_2 on c-MDF (blank: toluene standard without sample)

In general, anatase-type TiO_2 has a high photocatalytic activity because it shows higher oxidizing activity than the rutile structure. However, the 100 °C-treated TiO_2, which mainly comprised the rutile phase, also showed moderate photocatalytic activity. According to Wang *et al*. (2007), rutile-type TiO_2 showed good photocatalytic activity at the nanoscale. In this experiment, the synthesized rutile-type TiO_2 had an average length of 72 ± 14 nm and width of 14 ± 5 nm. Therefore, nanoscale rutile-type TiO_2 also could be used as a photocatalyst, although it was less effective than anatase-type TiO_2.

The same samples were repeatedly tested under the same conditions for 14 weeks to examine the reusability and persistency of the toluene decomposition performance of the c-MDF treated with the synthesized sol-type TiO_2. The sol-type TiO_2/c-MDF decomposed 20 ppm of toluene in the 20-L chamber within 7 h to 8 h in each test (14 times) over 14 weeks; therefore, treated c-MDF could be applied as an interior material to improve indoor air quality (Fig. 12).

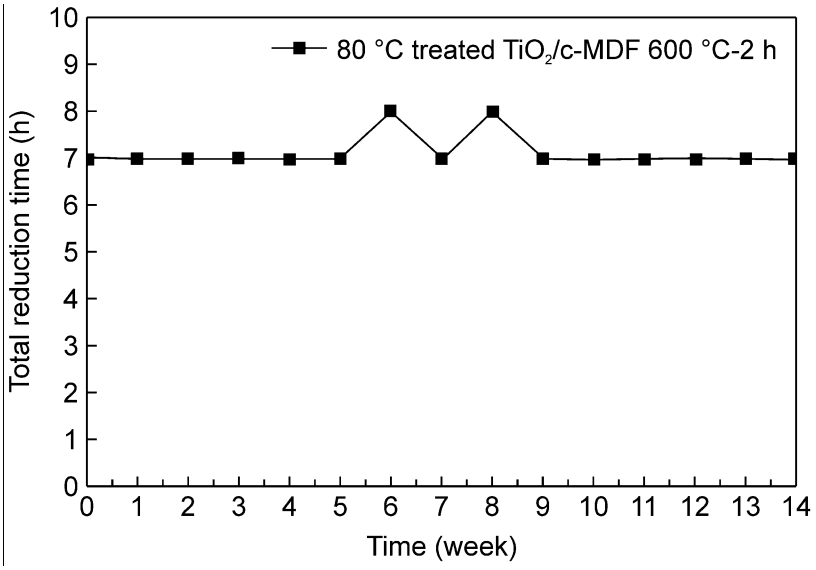

Fig. 12. Persistency of sol-type TiO_2-applied c-MDF for toluene decomposition over 14 weeks

CONCLUSIONS

1. Sol-type TiO_2 photocatalysts (3%) were synthesized using a modified sol-gel method in alcohol (IPA or EtOH) or water. In the TiO_2 synthesis, the lower alcohols, such as IPA and EtOH, were unsuitable for the formation of crystalline TiO_2. The water condition favored the formation of anatase-type crystalline TiO_2.
2. The most important factor in the water synthesis of anatase-type TiO_2 was the hydrothermal treatment temperature. The XRD analysis of the TiO_2 showed that anatase-type TiO_2 could be produced with hydrothermal treatment at 80 °C, while mostly rutile-type TiO_2 was formed in hydrothermal treatments at temperatures below 80 °C or above 90 °C.
3. Based on Ti mapping analysis using SEM-EDS, the TiO_2 was uniformly distributed on the surface of c-MDF.
4. The sol-type TiO_2 on c-MDF showed outstanding toluene decomposition performance (100% degradation of 20 ppm toluene within 7 h to 8 h) with good performance maintenance for 14 weeks.

REFERENCES CITED

Andersson, M., Österlund, L., Ljungström, S., and Palmqvist, A. (2002). "Preparation of nanosize anatase and rutile TiO_2 by hydrothermal treatment of microemulsions and their activity for photocatalytic wet oxidation of phenol," *J. Phys. Chem. B.* 106(41), 10674-10679. DOI: 10.1021/jp025715y

Ao, C. H., and Lee, S. C. (2004). "Combination effect of activated carbon with TiO_2 for the photodegradation of binary pollutants at typical indoor air level," *J. Photoch. Photobio. A* 161(2-3), 131-140. DOI: 10.1016/S1010-6030(03)00276-4

Bazargan, M. H., Byranvand, M. M., and Kharat, A. N. (2012). "Preparation and characterization of low temperature sintering nanocrystalline TiO_2 prepared *via* the sol-gel method using titanium (IV) butoxide applicable to flexible dye sensitized solar cells," *Int. J. Mater. Res.* 103(3), 347-351. DOI: 10.3139/146.110644

Byranvand, M., Kharat, A. N., Fatholahi, L., and Beiranvand, Z. M. (2013). "A review on synthesis of nano-TiO_2 *via* different methods," *Journal of Nanostructures* 3(1), 1-9. DOI: 10.7508/jns.2013.01.001

Centers for Disease Control and Prevention (CDC) (2006). *Healthy Housing Reference Manual*, U.S. Department of Health and Human Services, Atlanta, GA.

Corradi, A. B., Bondioli, F., Focher, B., Ferrari, A. M., Grippo, C., Mariani, E., and Villa, C. (2005). "Conventional and microwave-hydrothermal synthesis of TiO_2 nanopowders," *J. Am. Ceram. Soc.* 88(9), 2639-2641. DOI: 10.1111/j.1551-2916.2005.00474.x

Doi, M., Saka, S., Miyafuji, H., and Goring, D. A. (2000). "Development of carbonized TiO_2-woody composites for environmental cleaning," *Mater. Sci. Res. Int.* 6(1), 15-21.

Field, R. W. (2010). *Climate Change and Indoor Air Quality*, U. S. Environmental Protection Agency, Office of Radiation and Indoor Air, Raleigh, NC, USA.

Fujishima, A., Rao, T. N., and Tryk, D. A. (2000). "Titanium dioxide photocatalysis," *J. Photoch. Photobio. C* 1(1), 1-21. DOI: 10.1016/S1389-5567(00)00002-2

Guo, H., Lee, S. C., Chan, L. Y., and Li, W. M. (2004). "Risk assessment of exposure to volatile organic compounds in different indoor environments," *Environ. Res.* 94(1), 57-66. DOI: 10.1016/S0013-9351(03)00035-5

Hashimoto, K., Irie, H., and Fujishima, A. (2005). "TiO_2 photocatalysis: A historical overview and future prospects," *Jpn. J. Appl. Phys.* 44(12), 8269-8285 DOI: 10.1143/JJAP.44.8269

Kercher, A. K., and Nagle, D. C. (2002). "Evaluation of carbonized medium-density fiberboard for electrical applications," *Carbon* 40(8), 1321-1330. DOI: 10.1016/S0008-6223(01)00299-8

Kim, Y. S. (1999). "Present and future perspectives of studies on indoor air quality," *J. Korean Soc. Atmos. Environ.* 15(4), 371-383.

Lee, M., Park, S. B., and Lee, S. M. (2014). "Effect of carbonization temperature on hygric performance of carbonized fiberboards," *J. Korean Wood Sci. Technol.* 42(5), 615-623. DOI: 10.5658/WOOD.2014.42.5.615

Lee, M., Jang, J. H., Lee, S. M., and Park, S. B. (2017a). "Comparison of the radon absorption capacity of carbonized boards from different wood-based panels," *BioResources* 12(3), 6427-6433. DOI: 10.15376/biores.12.3.6427-6433

Lee, M., Jang, J. H., Lee, S. M., and Park, S. B. (2017b). "Effect of loess treatment and carbonization on the hygric performance of medium-density fiberboard," *BioResources* 12(3), 6418-6426. DOI: 10.15376/biores.12.3.6418-6426

Molinari, R., Mungari, M., Drioli, E., Dipaola, A., Loddo, V., Palmisano, L., and Schiavello,

M. (2000). "Study on a photocatalytic membrane reactor for water purification," *Catal. Today* 55(1-2), 71-78. DOI: 10.1016/S0920-5861(99)00227-8

Park, S. B., Lee, S. M., Park, J. Y., and Lee, S. H. (2009). "Manufacture of crack-free c-MDF from fiberboard," *Mokchae Konghak [Wood Science & Technology]* 37(4), 293-299.

Takeda, N., Torimoto, T., Sampath, S., Kuwabata, S., and Yoneyama, H. (1995). "Effect of inert supports for titanium dioxide loading on enhancement of photodecomposition rate of gaseous propionaldehyde," *J. Phys. Chem.* 99(24), 9986-9991. DOI: 10.1021/j100024a047

Tokoro, H., and Saka, S. (2001). "The photo-catalytic mechanism for formaldehyde by carbonized TiO_2-woody composites," *J. Soc. Mater. Sci. Jpn.* 50(6Appendix), 132-137. DOI: 10.2472/jsms.50.6Appendix_132

Torimoto, T., Okawa, Y., Takeda, N., and Yoneyama, H. (1997). "Effect of activated carbon content in TiO_2-loaded activated carbon on photodegradation behaviors of dichloromethane," *J. Photoch. Photobio. A* 103(1-2), 153-157. DOI: 10.1016/S1010-6030(96)04503-0

United State Environmental Protection Agency (US EPA) (2010). "Indoor air pollution: An introduction for health professionals," (http://www.epa.gov/iaq/pubs/hpguide.html), Accessed 5 Nov 2017.

Wahi, R. K., Liu, Y., Falkner, J. C., and Colvin, V. L. (2006). "Solvothermal synthesis and characterization of anatase TiO_2 nanocrystals with ultrahigh surface area," *J. Colloid Interf. Sci.* 302(2), 530-536. DOI: 10.1016/j.jcis.2006.07.003

Wang, D., Yu, B., Zhou, F., Wang, C., and Liu, W. (2009). "Synthesis and characterization of anatase TiO_2 nanotubes and their use in dye-sensitized solar cells," *Mater. Chem. Phys.* 113(2), 602-606. DOI: 10.1016/j.matchemphys.2008.08.011

Wang, Y., Zhang, L., Deng, K., Chen, X., and Zou, Z. (2007). "Low temperature synthesis and photocatalytic activity of rutile TiO_2 nanorod superstructures," *J. Phys. Chem.* 111(6), 2709-2714. DOI: 10.1021/jp066519k

Wen, B., Liu, C., and Liu, Y. (2005). "Depositional characteristics of metal coating on single-crystal TiO_2 nanowires," *J. Phys. Chem. B* 109(25), 12372-12375. DOI: 10.1021/jp050934f

Wu, J. M., and Qi, B. (2007). "Low-temperature growth of a nitrogen-doped titania nanoflower film and its ability to assist photodegradation of rhodamine B in water," *J. Phys. Chem. C* 111(2), 666-673. DOI: 10.1021/jp065630n

Xue, B., Sun, T., Mao, F., Sun, L. C., Yang, W., Xu, Z. D., and Zhang, X. (2011). "Facile synthesis of mesoporous core-shell TiO_2 nanostructures from $TiCl_3$," *Mater. Res. Bull.* 46(9), 1524-1529. DOI: 10.1016/j.materresbull.2011.05.019

Zhang, Q., and Gao, L. (2003). "Preparation of oxide nanocrystals with tunable morphologies by the moderate hydrothermal method: insights from rutile TiO_2," *Langmuir* 19(3), 967-971. DOI: 10.1021/la020310q

Zhou, Y., Huang, Y., Li, D., and He, W. (2013). "Three-dimensional sea-urchin-like hierarchical TiO_2 microspheres synthesized by a one-pot hydrothermal method and their enhanced photocatalytic activity," *Mater. Res. Bull.* 48(7), 2420-2425. DOI: 10.1016/j.materresbull.2013.02.051

Article submitted: March 15, 2019; Peer review completed: June 16, 2019; Revised version received: June 20, 2019; Accepted: June 21, 2019; Published: June 26, 2019.
DOI: 10.15376/biores.14.3.6516-6528